Cancer Management and Research

Dovepress

open access to scientific and medical research

Open Access Full Text Article

ORIGINAL RESEARCH

RETRACTED ARTICLE: LncRNA EMX2OS Induces Proliferation, Invasion and Sphere Formation of Ovarian Cancer Cells via Regulating the miR-654-3p/AKT3/PD-L1 Axis

This article was published in the following Dove Press journal:
Cancer Management and Research

Meng Duan*
Meixia Fang*
Changhe Wang
Hongyan Wang
Meng Li

Department of Gynecology, Jining No. 1 People's Hospital, Jining, Shandong 272000, People's Republic of China

*These authors contributed equally to this work

Purpose: Long noncoding RNA (lncRNA) dereg ulation is frequent in human ovarian cancers (OCs), but the role of specific miRNA involv in this disease remains elusive. LncRNA EMX2OS was previously repo d to as an on gene in human cancers. However, their accurate expression, fun on and unde ing mechanisms in OC are largely unclear.

Materials and Methods: The levels of EM 2OS in OC tissues and cell lines were determined by quantitative r l-time PCR, and the nction of EMX2OS was then analyzed both in vitro and in vivo. L ciferase assay and immunoprecipitation assays were performed to analyze the association tween EMX2 S and miR-654 expression in OC cells.

Results: EMX2OS is over ressed i human ovarian cancer tissues. Knockdown of EMX2OS reduc via overexpression of EMX2OS enhanced the proliferation, invasion and sphere forma n of lls. In addition, EMX2OS enhanced tumor growth in an in vivo graft m l of human OC. We discovered that EMX2OS directly binds to miR-654 d sup esses its xpression, thus leading to the upregulation of AKT3, which served as direct ta t of miR 54. Moreover, miR-654 inhibited cell proliferation, invasion and sph formation, and restoration of AKT3 reversed the effects of EMX2OS silencing or miR-65 verexpression. Furthermore, PD-L1 was identified as the key oncogenic component acting downstream of AKT3 in OC cells. Ectopic expression of PD-L1 reversed the anti-cancer functions by EMX2OS knockdown, AKT3 silencing or miR-654 upregulation in OC lls.

Conclusion: These results demonstrated that the EMX2OS/miR-654/AKT3/PD-L1 axis confers aggressiveness in ovarian cancer and may represent a therapeutic target for OC metastasis.

Keywords: EMX2OS, ovarian cancer, AKT3, microRNA-654, PD-L1

Introduction

Ovarian cancer (OC) is the most lethal gynecological cancer, accounting for ~2.5 and 5% of female cancer occurrences and deaths worldwide.[1] It is difficult to diagnose ovarian cancer at an early stage, because early-stage OC often has no symptoms.[2] More than 70% of women with OC are diagnosed with advanced disease. A 5-year survival rate for women with advanced disease is approximately 20% to 30%.[3] Although tremendous efforts had been made to seek novel biomarkers for identifying OC tumors at early stages or build better therapeutic approaches for treatments, there has been little progress on improving OC patients' prognosis.[3]

Correspondence: Meng Li
Department of Gynecology, Jining No. 1 People's Hospital, Jining, Shandong 272000, People's Republic of China
Tel +86 537 2253304
Email limeng_19@yahoo.co.jp

submit your manuscript | www.dovepress.com
DovePress
http://doi.org/10.2147/CMAR.S229013

Many molecular mechanisms have been identified to play critical roles in regulating pathogenesis, metastasis and chemoresistance of OC.[4] Among them, non-coding RNAs, which contain microRNA (miRNA) and long non-coding RNA (lncRNA), were shown to be dysregulated in OC and have been recognized as new targets of treatments in many tumors.[5,6] In cancer cells, miRNAs regulate the gene expression post-transcriptionally by binding to mRNA 3′-untranslated region (3′-UTR), leading to translational repression or mRNA degradation.[7] Recent studies have demonstrated that lncRNA EMX2OS was significantly upregulated in gastric cancer tissues compared to the matched control tissues.[8] However, the expression, effects and mechanisms of EMX2OS in OC remain largely unknown.

In the present work, we attempted to explore the expression, cellular function and potential mechanisms of EMX2OS in OC. Our results suggested that EMX2OS was overexpressed in OC tissues and OC cell lines. Gain- and loss-of-function analysis showed the tumor-promoting role of EMX2OS in vitro and in vivo. Finally, our mechanistic analysis indicated that EMX2OS promotes proliferation, invasion and sphere formation of OC cells via regulating the AKT3/PD-L1 axis by sponging miR-654. Thus, the EMX2OS/miR-654/AKT3 axis seems to be a promising therapeutic target for OC.

Materials and Methods

Cell Lines and Transfection

Human OC cell lines (SKOV-3, ES-2, OVCAR3, A2780, CAOV3, American Type Culture Collection, Rockville, USA) and normal human ovary cell line IOSE-80 (Chinese Academia of Sciences, Shanghai, China) were cultured in DMEM/F12 medium (Gibco, Grand Island, NY, USA) supplemented with 10% of fetal bovine serum (FBS). The transfection plasmid for lncRNA-EMX2OS, AKT3, PD-L1 and respective control plasmid were constructed by Genepharma (Shanghai, China). EMX2OS siRNAs, PD-L1 siRNAs, AKT3 siRNAs, control siRNA, miR-654 mimic, control mimic, miR-654 inhibitor and control inhibitor were purchased from Genepharma (Shanghai, China). Lipofectamine 2000 (Invitrogen, Carlsbad, CA, USA) was employed for cell transfection following the guidance of the manufacturer's instructions. The efficiency of transfection was assessed at 48 hrs after transfection by visualizing uptake of the BLOCK-iT Fluorescent Oligo (Thermo Fisher Scientific, Waltham, MA, USA) using fluorescence microscopy (Figure S1), as previously reported.[9]

qRT-PCR Analysis

Total RNA was isolated using TRIzol reagent (Invitrogen, Carlsbad, CA, USA) according to the manufacturer´s instructions. Complementary DNA was synthesized with a Reverse Transcription Kit (Takara, Dalian, China). The levels of EMX2OS and GAPDH were quantified using the SYBR-Green-quantitative real-time PCR Master Mix kit (Toyobo, Osaka, Japan). The NCode miRNA qRT-PCR kit (Invitrogen, Carlsbad, CA, USA) was used to detect the miR-654 level according to the manufacturer's instructions. The primers for EMX2OS, *Caspase-3, Nanog, Sox2, Oct4, GAPDH*, miR-654 and U6 were obtained from RiboBio (Guangzhou, China). The primer sequences used are as follows: *EMX2OS* (forward: 5′-gtgacttgcacaaggacaaa-3′, reverse: 5′-tgtvtggccattcctct-3′); *Caspase-3* (forward: 5′-tctggtgggtgtg-3′, reverse: 5′-cgcttccatgtatgatctttgg-3′), *Nanog* (forward: 5′-accttg gctgccg-3′, reverse: 5′-agcaaagcctcccaatcccaaaca-3′), *Sox2* (forward: 5′-gagctttgcaggaagtttgc-3′, reverse: 5′-gcaaagcctctccttga-3′), *Oct4* (forward: 5′-ttttggtacccc aggc-3′, reverse: 5′-gcaggcacctcagtttgaat-3′), *GAPDH* (forward: cacatcgctcagacac-3′, reverse: 5′-gcccaat acatcc-3′), miR-654 (forward: 5′-tatgtctgctgac atcacctt-3′, reverse: provided in the NCode miRNA qRT-PCR kit) and U6 (forward: 5′-acgcaaattcgtgaagcgtt-3′, reverse: provided in the NCode miRNA qRT-PCR kit). *GAPDH* or U6 were used as the endogenous control for EMX2OS or miR-654, respectively. The relative expression of gene and miRNA was analyzed using the $2^{-\Delta\Delta Ct}$ method.

MiRNA Stability Assay

Cells were seeded in 12-well plates and cultured at 37 °C under 5% CO_2 for 24 hrs. Total RNA was isolated from cells treated with 10 μg/mL Actinomycin D (Sigma-Aldrich, Louis, MO, USA) at 0, 12 and 24 hrs respectively. Relative abundance of miRNAs was detected by qRT-PCR analysis.

Western Blotting Analysis

Total protein from cells was isolated by using RIPA lysis buffer (Pierce, Rockford, IL, USA). The protein sample was subjected to 10% sodium dodecyl sulfate-polyacrylamide gel electrophoresis (SDS-PAGE) and then transferred to a nitrocellulose membrane (Bio-Rad, Hercules, CA, USA). Following blocking with 5% nonfat milk at room temperature for 1h, the immunoblots was incubated with the

primary antibody against AKT3 (1:1000, Santa Cruz Biotech, Santa Cruz, CA), PD-L1 (1:1000, Proteintech, Chicago, IL, USA) and GAPDH (1:1000, Santa Cruz Biotech, Santa Cruz, CA). Subsequently the membranes were incubated with the appropriate secondary antibodies, and the protein signals were determined using the ECL detection kit (Pierce Biotechnology, Rockford, IL, USA). The expression of GAPDH was used as an endogenous loading control.

Cell Counting Kit-8 (CCK-8) Assay

Cell proliferation was measured by CCK-8 (Beyotime Institute of Biotechnology, Jiangsu, China) according to the manufacturer's instructions. Briefly, OC cells (100 μL of culture medium/well) were seeded into 96-well plates and transfected as indicated. After incubation for 72 hrs, 10 μL CCK-8 solutions were added to each well of the 96-well plates. The absorbance was measured at 450 nm by a microplate reader (Bio-Rad, Hercules, CA, USA).

Sphere-Forming Assay

Cells were transfected with EMX2OS siRNA or EMX2OS expression vector, respectively. After 48 hrs, 2500 cells were plated on ultra-low attachment plates (Corning, NY, USA) in serum-free DMEM-F12 medium (Gibco, Grand Island, NY, USA) supplemented with 20 ng/mL EGF (Invitrogen, Carlsbad, CA, USA), 20 ng/mL FGF (Invitrogen, Carlsbad, CA, USA) 4 mg/mL heparin (Sigma-Aldrich, Taufkirchen, Germany), and 2% B27 (Invitrogen, Carlsbad, CA, USA). After 14 days, the sphere number and size were analyzed by ImageJ software.

Cell Invasion Assay

The 24-well transwell chambers coated with Matrigel (Corning, New York, USA) were used to assess the invasiveness of OC cells as described previously.[10] OC cells (5×10^4 per well) were suspended onto the top of the invasion chambers. The lower chambers were filled with the medium containing 10% FBS as chemo-attractant. After 24 hrs incubation, the noninvasive cells inside the upper chambers were scraped off with cotton swabs, and the invading cells on the lower membrane surface were fixed with 75% methanol and then stained with 20% Giemsa. Cells were photographed and counted in five random fields for each chamber.

Luciferase Reporter Assay

The wild-type fragment of EMX2OS (EMX2OS-WT), mutant EMX2OS (EMX2OS-MUT), wild-type *AKT3* 3′-UTR (AKT3-WT), and mutant *AKT3* 3′-UTR (AKT3-MUT) were synthesized and constructed into pGL3 luciferase reporter vector (Promega, Madison, WI, USA). OC cells were seeded into 96-well plates, and 1 day later the above luciferase reporter vectors (100 ng) containing EMX2OS (WT or MUT) or *AKT3* 3′-UTR (WT or MUT) were co-transfected with miR-654 mimic, miR-654 inhibitor or their respective controls (50 nM) into OC cells, along with Renilla luciferase plasmid (10 ng, pRL-CMV, Promega, WI, USA) used for normalization. Lipofectamine 2000 (Invitrogen, Carlsbad, CA, USA) was used as transfection agent following the manufacturer's protocol. Cells were harvested 48 hrs after transfection and the luciferase activity was measured using the Dual-luciferase reporter assay kit (Promega, China) according to the manufacturer's instructions. Firefly luciferase activity was normalized to that of Renilla luciferase.

RNA Immunoprecipitation Assay (RIP)

RNA immunoprecipitation assay was performed using the Magna RIP™ RNA-Binding Protein Immunoprecipitation Kit (Millipore, Bedford, MA, USA). In brief, OC cells at 80% confluency were harvested and lysed in complete RIP lysis buffer on ice for 10 min. The lysates were pre-cleared by centrifugation, and 50 μL the samples were aliquoted for input. The remaining lysates were incubated with RIP buffer containing magnetic beads conjugated with anti-Argonaute2 (Ago2) antibody (Millipore) or normal mouse IgG (Millipore) as a negative control. Samples were digested with proteinase K, and the bound RNAs were isolated and subjected to qRT-PCR analysis of EMX2OS and miR-654 expression.

Xenograft Mouse Model

All experiment protocols were approved by the Institutional Animal Care and Ethics Committee of Jining No. 1 People's Hospital, and the animals were cared for in agreement with Institutional ethics guidelines. Four-week-old BALB/c nude mice were purchased from Beijing Vital Laboratory Animal Technology (Beijing, China). For subcutaneous xenograft tumour assay, a total of 2×10^6 OC cells per mouse were subcutaneously injected into in the right flank of the nude mice. OC cells were injected into subcutaneously in the flank of the nude mice. Tumors were measured using a caliper, and tumor volume (mm^3) was calculated using the following formula: length × width^2 × 0.5. 3 weeks after injection, the mice

were sacrificed, and the tumors were collected for further analysis. Serial 6.0 μm sections were cut and subjected to immunohistochemistry assay using an anti-Ki67 antibody (Abcam, Cambridge, UK).

Tissue Specimens

The study was approved and performed in accordance with the guideline of the independent Ethics Committee of Jining No. 1 People's Hospital, and informed consents were signed by all patients prior to participation in the study. A total of 50 patients undergoing resection of the primary ovarian serous adenocarcinomas at Jining No. 1 People's Hospital were enrolled in this study. Inclusion criteria were as follows: (1) tumor histology originating from epithelial tissue, (2) staging according to the International Federation of Gynecology and Obstetrics, (3) defined surgical strategies, and (4) OC tissues and paired adjacent tissues were available. OC patients with the following characteristics were excluded: (1) treatment with chemotherapy, (2) treatment with radiotherapy, (3) treatment with immunotherapy prior to surgery, and (4) history of other solid tumors or hematological malignancies. The normal paired tissues were taken from the distal resection margins (more than 5 cm). All tissue specimens obtained were confirmed by pathologists. Tumor tissues and adjacent noncancerous tissues were collected for RNA extraction and qRT-PCR assays.

Statistical Analysis

All statistical analyses were done with SPSS 20.0 statistical software (IBM, Chicago, USA). Data are presented as the mean ± standard deviation based on at least three repeats. The significant differences were assessed using Student's *t*-test, one-way ANOVA and Wilcoxon signed-rank test. $P < 0.05$ from a two-tailed test was considered as statistically significant.

Results

EMX2OS Is Overexpressed in OC Tissues and OC Cell Lines and Upregulation of EMX2OS Is Correlated with Poor Survival

To explore the role of lncRNA EMX2OS in OC, we first analyzed the expression of EMX2OS in TCGA OC dataset using the cBioPortal portal (http://cbioportal.org). We found that EMX2OS was amplified and overexpressed in OC patients (Figure 1A). We also explored the expression of EMX2OS in OC tissues and normal ovarian tissues from GEPIA (http://gepia.cancer-pku.cn/), an interactive web-based TCGA database.[11] As shown in Figure 1B, the elevated expression of EMX2OS was observed in OC tissues compared with non-tumor ovary tissues. To validate the TCGA analysis results, we measured the expression of EMX2OS in 50 paired OC samples and paired normal samples. The qRT-PCR results demonstrated that EMX2OS levels were significantly higher in OC tissues compared to normal tissues (Figure 1C).

Then, we measured the expression of EMX2OS in five OC cell lines (SKOV-3, OVCAR3, A2780, CAOV3 and ES-2) and human normal ovary cell line ISOE-80. Our results indicated that EMX2OS expression was significantly higher in OC cells than in ISOE-80 cells (Figure 1D). Furthermore, we performed survival analysis using the Kaplan Meier Plotter database (http://kmplot.com/analysis). Samples are split into two groups using median value across the entire dataset. The results showed that higher EMX2OS expression predicted poor survival in OC patients (Figure 1E). Thus, these data demonstrate that EMX2OS expression is increased in OC tissues and cell lines, and high EMX2OS expression correlates with poor survival of patients with OC.

Knockdown of EMX2OS Inhibits OC Cell Proliferation, Invasion and Sphere Formation

To investigate the potential role of EMX2OS in OC development, we silenced EMX2OS expression in ES-2 cells by transfection with EMX2OS-specific siRNAs. As shown in Figure 2A, cells transfected with EMX2OS siRNAs showed an obviously reduced expression of EMX2OS compared with the control cells. The results of CCK-8, invasion and sphere formation assays suggested that knockdown of EMX2OS significantly suppressed the proliferation, invasion and sphere formation of ES-2 cells (Figure 2B–D). We also evaluated the effects of EMX2OS upregulation on proliferation, invasion and sphere formation in another OC cell line SKOV-3 (Figure 2A). Compared with the control cells, the transfection with EMX2OS expression vector led to a significant increase in proliferation, invasion and sphere formation of SKOV-3 cells (Figure 2B–D). Moreover, we found that overexpression of EMX2OS increased the proliferation and invasion of OVCAR3 cells, and downregulation of EMX2OS reduced these malignant properties in A2780 cells (Figure S2).

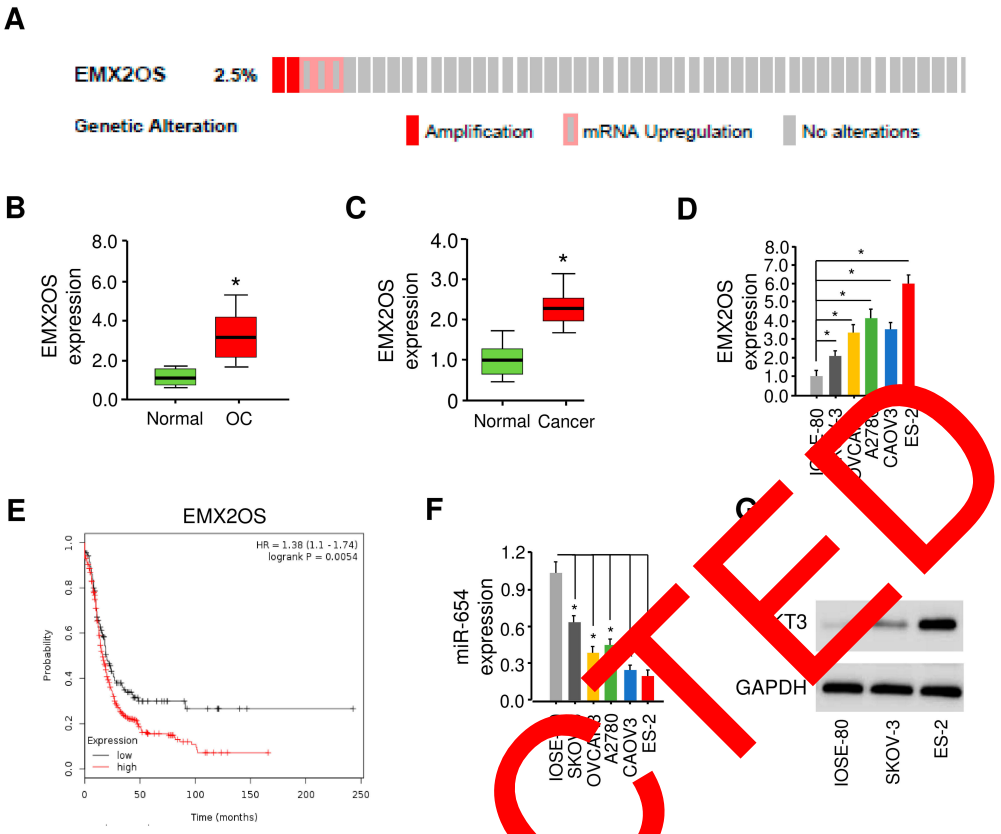

Figure 1 EMX2OS is overexpressed in OC tissues and OC cell lines and [illegible] correlated with poor survival. (**A**) The cBioPortal result shows that EMX2OS was amplified in 585 patients obtained from TCGA-OC dataset. (**B**) [illegible] of EMX2OS in OC samples (n = 70) and normal ovarian tissues (n = 20). The Cancer Genome Atlas (TCGA) datasets were retrieved from the GEPIA database (http[illegible]cancer-pku.cn/). (**C**) qRT-PCR analysis of EMX2OS in OC samples (n = 50) and normal samples (n = 50). (**D**) qRT-PCR analysis of EMX2OS in OC cell lines and [illegible] ovary cell IOSE-80. (**E**) Kaplan–Meier curves for overall survival were created using the Kaplan–Meier Plotter with OC patients classified according to [illegible] and low EMX2OS expression. (**F**) miR-654 expression in OC cell lines and normal ovary cell IOSE-80. (**G**) Western blot analysis of AKT3 expression in OC cell lines and normal ovary cell IOSE-80. *$P<0.05$.
Abbreviations: OC, ovarian cancer; TCGA, the cancer genome atlas; qRT-PCR, quantitative PCR.

Using qRT-PCR assays, we confirmed that the levels of *Caspase-3* was significantly increased after the knockdown of EMX2OS in ES-2 cells, while was significantly repressed after the overexpression of EMX2OS in SKOV-3 cells (Figure 2E). Interestingly, our qRT-PCR experiments showed that knockdown of EMX2OS significantly suppressed the expression of *Nanog, SOX2* and *Oct4* in ES-2 cells, and overexpression of EMX2OS significantly increased the expression of *Nanog, SOX2* and *Oct4* in SKOV-3 cells (Figure 2E). These data collectively suggest that upregulation of EMX2OS has significant oncogenic effects on OC growth, invasion and sphere formation.

EMX2OS Enhances Tumor Growth in a Mouse Xenograft Models

Next, we further investigated the effect of EMX2OS on OC proliferation using a nude mice xenograft tumor model. ES-2 cells were transfected with EMX2OS siRNAs or control siRNA, and SKOV-3 cells were transfected with EMX2OS expression vector or control vector before subcutaneous implantation. Silencing of EMX2OS significantly decreased tumor growth, as observed by the smaller tumor sizes of EMX2OS siRNAs-transfected tumors compared to the control siRNA-transfected tumors (Figure 3A). On the other hand, overexpression of EMX2OS dramatically induced tumor size compared with control group (Figure 3B). In addition, immunohistochemical analysis revealed that the tumor tissues of the EMX2OS knockdown groups displayed much weaker staining of Ki-67 (Figure 3C). Importantly, Ki-67 expression was increased in the tumor tissues of EMX2OS overexpression group mice (Figure 3D). Taken together, these results clearly suggest that EMX2OS could enhance OC proliferation in vivo.

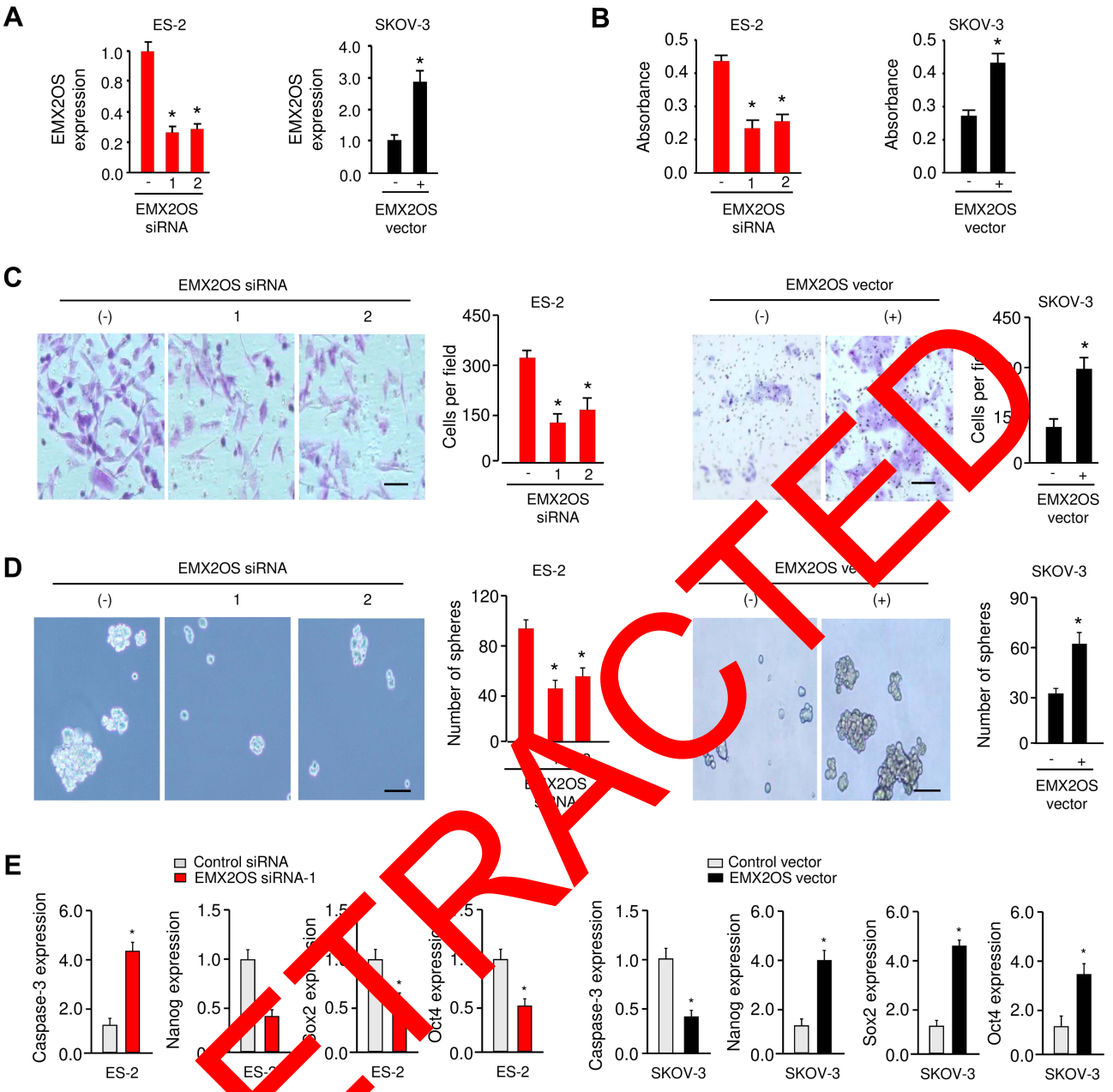

Figure 2 EMX2OS promoted proliferation, sphere formation and invasion of OC cells. (**A**) qRT-PCR analysis of EMX2OS expression in ES-2 cells transfected with EMX2OS siRNA or control siRNA, and in SKOV-3 cells transfected with EMX2OS vector or control vector. (**B**) Overexpression of EMX2OS promoted the proliferation as measured by CCK-8 assay. (**C**) Transwell invasion assay was used to examine invasiveness in EMX2OS-knockdown ES-2 cells (left), and in SKOV-3 cells overexpressing EMX2OS (right, magnification, × 100). Scale bar, 50 μm. (**D**) Sphere formation assays in ES-2 cells after knockdown of EMX2OS (left) and in SKOV-3 cells after overexpression of EMX2OS (right, magnification, ×100). Scale bar, 50 μm. (**E**) qRT-PCR analysis of *Caspase-3, Nanog, SOX2* and *Oct4* expression in ES-2 cells transfected with EMX2OS siRNA-1 or control siRNA (left), and in SKOV-3 cells transfected with EMX2OS vector or control vector (right). *$P<0.05$.
Abbreviations: OC, ovarian cancer; qRT-PCR, quantitative PCR; CCK-8, Cell Counting Kit-8.

EMX2OS Functions as a Competing Endogenous RNA by Sponging miR-654 in OC Cells

Previous studies have shown that lncRNA could act as a competing endogenous RNA to interact with miRNA.[12] The public algorithm StarBase V2.0 was used to predict the potential lncRNA-miRNA interactions. We found that EMX2OS has a putative binding site for miR-654 (Figure 4A). Moreover, our qRT-PCR results suggested that miR-654 was downregulated in OC cells compared with the normal cells (Figure 1F), suggesting that EMX2OS expression was inversely correlated with miR-654 expression in OC cells.

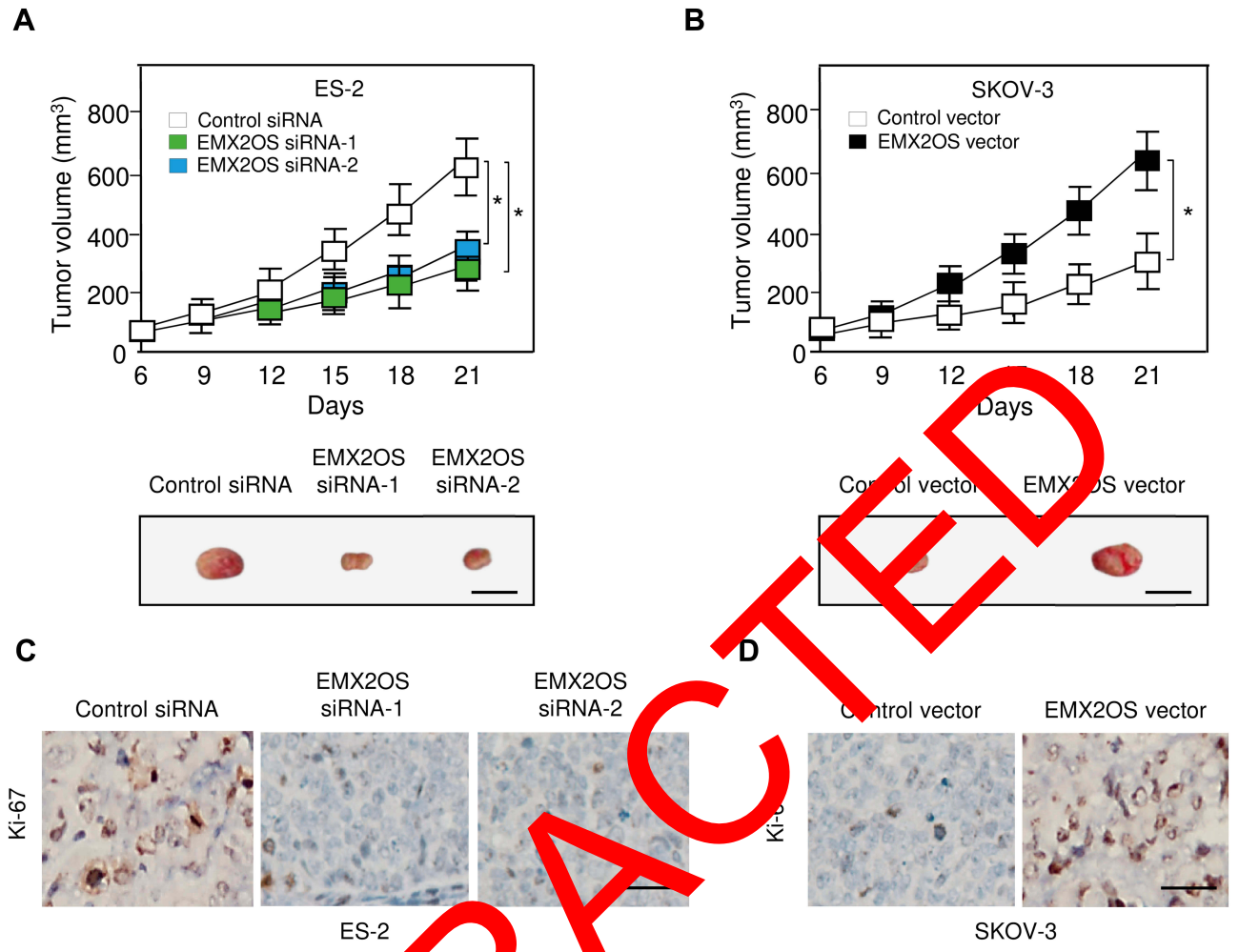

Figure 3 EMX2OS enhances tumor growth in a mou[se] xenogra[ft] (**A**, **B**) Comparison of tumor volume in ES-2 (**A**) cells transfected with EMX2OS siRNAs or control siRNA, or in SKOV-3 (**B**) cells transfected [with] EM[X2OS] vector or control vector (upper panel). Representative xenograft tumors derived from ES-2 or SKOV-3 cells (bottom panel, magnification, × 200). Scale ba[r] cm. (**C, D**) [Ki]-67 staining of tumor tissues from mice inoculated with ES-2 (**C**) cells transfected with EMX2OS siRNAs or control siRNA, or in SKOV-3 (**D**) cells tra[nsfect]ed with EMX2[OS] vector or control vector. Scale bar, 50 μm. *$P < 0.05$.

Previous reports suggested that oncogenic lncRNAs could promote cancer progression through inhibiting the expression of tumor suppressor miRNAs.[13,14] Moreover, lncRNA could suppress the expression of miRNA through inducing miRNA degradation.[15] To examine whether EMX2OS has any influence on miR-654 expression, qRT-PCR assays were used to investigate the expression of miR-654 in EMX2OS-knockdown ES-2 cells or in SKOV-3 cells overexpressing EMX2OS. The qRT-PCR results indicated that EMX2OS knockdown increased miR-654 expression, while EMX2OS overexpression decreased miR-654 expression (Figure 4B), suggesting that EMX2OS inhibits miR-654 expression in OC cells. The miRNA stability assay illustrated that ectopic overexpression of EMX2OS enhanced the degradation of miR-654, while knockdown of EMX2OS increased miR-654 stability (Figure 4C), suggesting that EMX2OS inhibits miR-654 expression by decreasing the stability of miR-654.

To determine the relationship between EMX2OS and miR-654, the dual-luciferase assay was performed. The ectopic expression of miR-654 significantly repressed the luciferase activity of wild-type EMX2OS, but not that of mutant EMX2OS in ES-2 cells (Figure 4D). Furthermore, we found that the inhibition of miR-654 induced the luciferase activity of EMX2OS-WT, but has no significant effects on the EMX2OS-MUT in SKOV-3 cells (Figure 4D). These data suggested that EMX2OS is a direct target of miR-654 in OC cells.

To test whether EMX2OS directly interacts with miR-654, we performed the RIP experiments. Our results showed that EMX2OS and miR-654 could be significantly enriched by Ago2 antibody compared with negative IgG (Figure 4E).

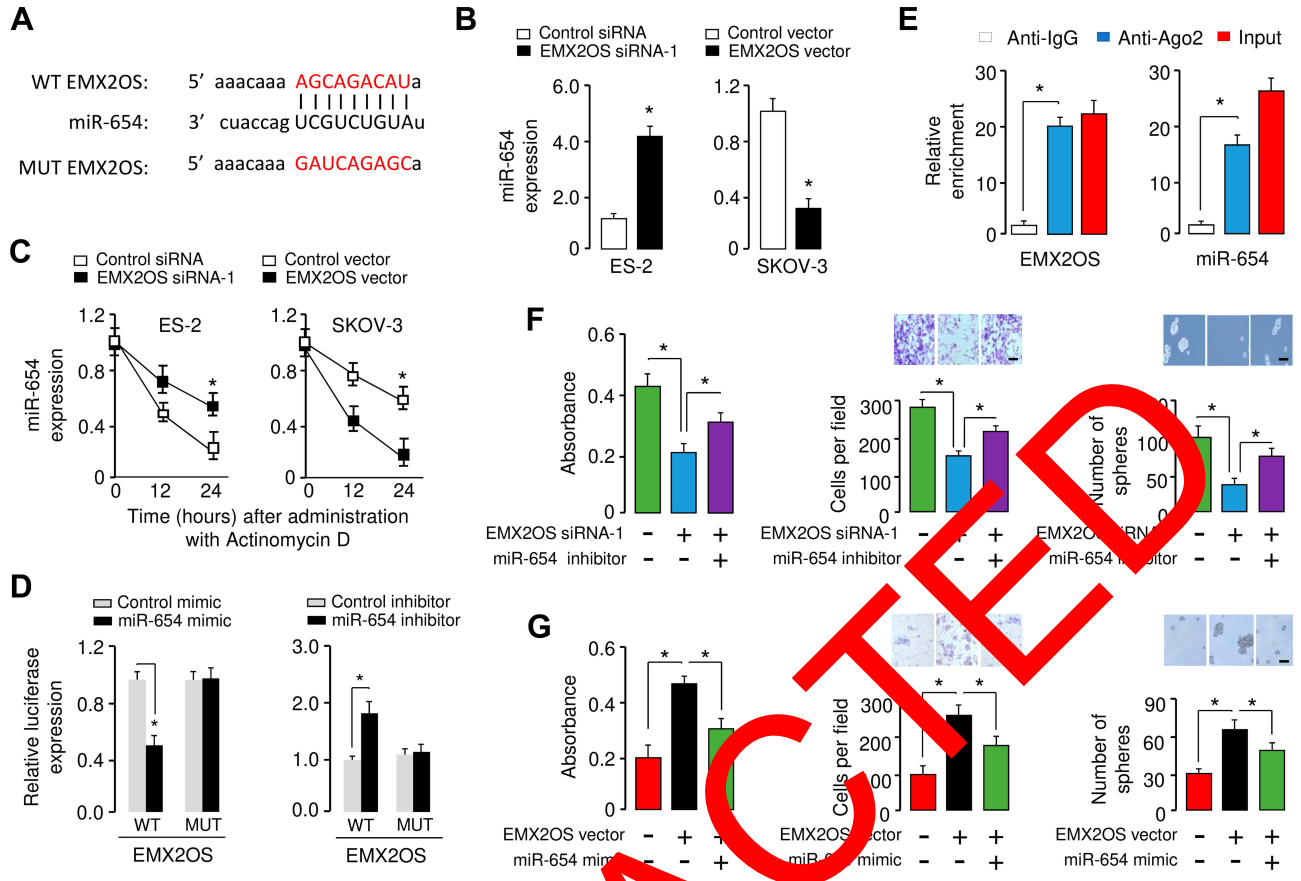

Figure 4 EMX2OS serves as a target of miR-654. (**A**) Putative miR-654 binding sit[illegible] EMX2[illegible]nce, with mutant sites shown in red. (**B**) qRT-PCR analysis showed that EMX2OS negatively regulated the expression of miR-654 in OC cells. (**C**) Stability [illegible] th[illegible]iR-654 after EMX2OS overexpression or knockdown. Levels of miR-654 were examined at different times after administration with Actinomycin[illegible]. The dua[illegible]iferase assay showed that miR-654 negatively regulated the luciferase activity of EMX2OS-WT, but has no significant effects on the EMX2OS-M[illegible]. (**E**) Th[illegible]ssociatio[illegible]etween EMX2OS and miR-654 was analyzed using RIP assay. (**F**) CCK-8, invasion and sphere formation assay were performed to determine ce[illegible]roliferatio[illegible]nvasion an[illegible]here formation of ES-2 cells transfected with EMX2OS siRNA or control siRNA, together with (or without) miR-654 inhibitor. (**G**) CCK-8, [illegible]asion a[illegible]rmation assay were performed to determine cell proliferation, invasion and sphere formation of SKOV-3 cells transfected with EMX2OS [illegible]tor or [illegible] vector, together with (or without) miR-654 mimic. *P<0.05.

Abbreviations: qRT-PCR, quantitative PCR; CCK-[illegible] Cell Counti[illegible]it-8.

We wondered whether miR-654 mi[illegible]t functionally affect the cancer-promo[illegible]g functions of EMX2OS in OC cells. We transfected E[illegible]X2O[illegible]siRNA together with miR-654 inhibitor int[illegible]ES-2 [illegible]ls, or [illegible]nsfected EMX2OS vector togeth[illegible] with [illegible]iR-654 [illegible]mic into SKOV-3 cells. Then, we p[illegible]formed [illegible]roliferation and invasion assays. We found tha[illegible]knockdown of EMX2OS significantly inhibited the prol[illegible]ation, invasion and sphere formation of ES-2 cells, and the inhibition of miR-654 significantly abrogated these effects (Figure 4F). Conversely, the overexpression of miR-654 could attenuate the promoting effects of EMX2OS on the proliferation, invasion and sphere formation in SKOV-3 cells (Figure 4G). Taken together, these results indicated that EMX2OS targets and suppresses the expression of miR-654 in OC cells by functioning as a competing endogenous RNA.

MiR-654 Directly Targets AKT3 in OC Cells

To investigate the potential mechanisms by which miR-654 inhibited OC cell growth and invasion, we searched TargetScan (http://www.targetscan.org) and selected AKT3 as a possible target of miR-654 (Figure 5A). To validate whether miR-654 could bind to the 3′-UTR of *AKT3*, we performed the luciferase assay and found that miR-654 overexpression significantly reduced the luciferase activity of the wild-type *AKT3* 3′-UTR, whereas the inhibition of miR-654 enhanced the luciferase activity of the wild-type *AKT3* 3′-UTR (Figure 5B). However, miR-654 expression did not change the luciferase activity of the mutant *AKT3* 3′-UTR (Figure 5B). Moreover, the Western blot analysis showed that miR-654 overexpression inhibited, while miR-654 inhibition increased the protein expression of AKT3 in OC cells (Figure 5C). We

explored the correlation between miR-654 and AKT3 in OC cells. Our Western blot experiments suggested that compared with that in normal cells, the expression of AKT3 in OC cells was much higher (Figure 1G). These findings support that AKT3 is a direct target of miR-654 in OC cells.

Introduction of AKT3 Reverses the Inhibitory Effects of EMX2OS Silencing and miR-654 Overexpression in OC Cells

We confirmed that knockdown of EMX2OS reduced the protein level of AKT3 in ES-2 cells, while the transfection with miR-654 inhibitor partially abolished this effect (Figure 5D). In contrast, overexpression of EMX2OS led to the upregulation of AKT3, and these effects could be largely reversed by the transfection with miR-654 mimic in SKOV-3 cells (Figure 5D), suggesting that EMX2OS positively regulated AKT3 expression by inhibiting miR-654 expression. Furthermore, the results of CCK-8, invasion and sphere formation assays demonstrated that knockdown of EMX2OS or miR-654 overexpression in ES-2 cells significantly repressed proliferation, invasion and sphere formation, while restoration of AKT3 expression partially reversed these anti-cancer effects induced by EMX2OS knockdown or miR-654 overexpression (Figure 6A–F).

Then, we found that *AKT3* was overexpressed at the mRNA level in 50 primary OC tissues compared with normal tissues (Figure 6G). To further validate the expression level of AKT3, we queried the Oncomine database (http://oncomine.com) for publically available OC microarray data and identified overexpression of AKT3 in the TCGA OC data set (Figure 6H). We then accessed the prognostic value of *AKT3* mRNA expression using the Kaplan Meier Plotter database. High *AKT3* mRNA expression was associated with significantly shorter overall survival for OC patients (Figure 6I). These data reveal that EMX2OS promotes OC cell proliferation, invasion and sphere formation by regulating the miR-654/AKT3 axis.

EMX2OS Promotes OC Cell Proliferation, Invasion and Sphere Formation via Regulating the AKT3/PD-L1 Axis by Sponging miR-654

Recent evidence has suggested that PD-L1, a key immune checkpoint molecule, has signal transduction capacities that contribute to tumor progression by regulating cell proliferation, migration, invasion and cancer stem cell expansion.[16] Since AKT3 was shown to function as an upstream activator of PD-L1 in breast cancer cells,[17] we tested whether the EMX2OS/miR-654/AKT3 axis promotes the aggressive phenotypes of OC cells in a PD-L1-dependent manner.

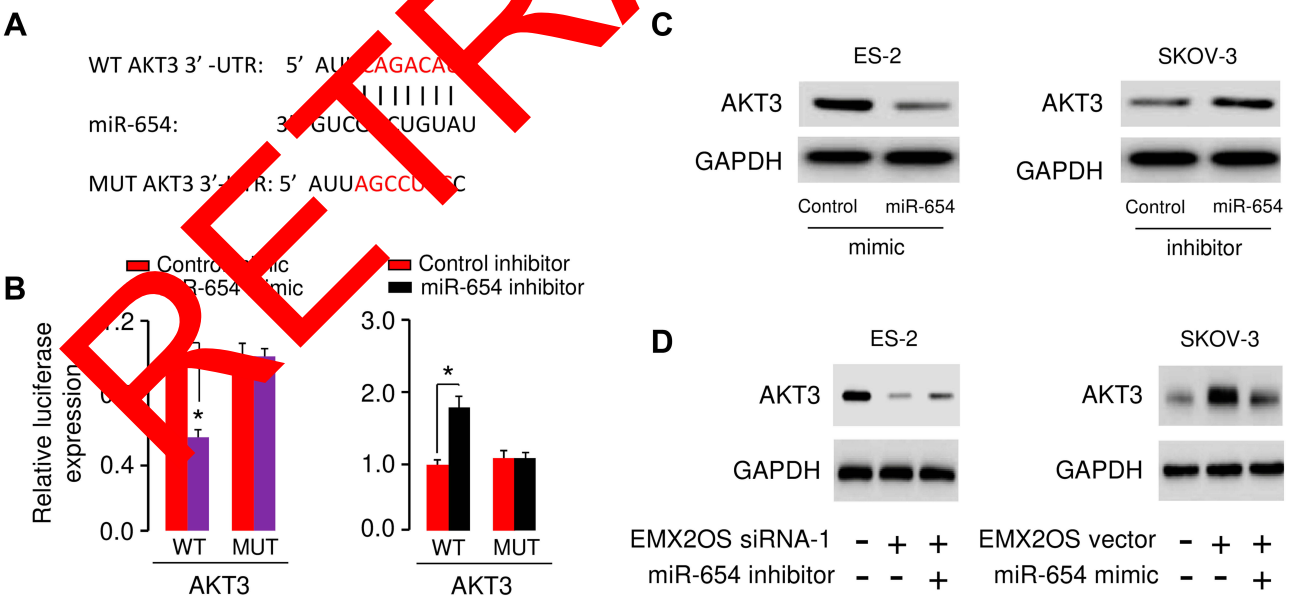

Figure 5 AKT3 is a direct target of miR-654. (**A**) Putative miR-654 binding site in the 3′-UTR of *AKT3*, with mutant sites shown in red. (**B**) The dual luciferase assay showed that miR-654 suppressed the luciferase activities of AKT3-WT, but not AKT3- MUT. (**C**) Western blot analysis of AKT3 in ES-2 cells transfected with miR-654 mimic or control mimic, and in SKOV-3 cells transfected with miR-654 inhibitor or control inhibitor. (**D**) The expression of AKT3 in ES-2 cells transfected with EMX2OS siRNA or control siRNA, together with (or without) miR-654 inhibitor, and in SKOV-3 cells transfected with EMX2OS vector or control vector, together with (or without) miR-654 mimic. *P<0.05.

Abbreviation: 3′-UTR, 3′-untranslated region.

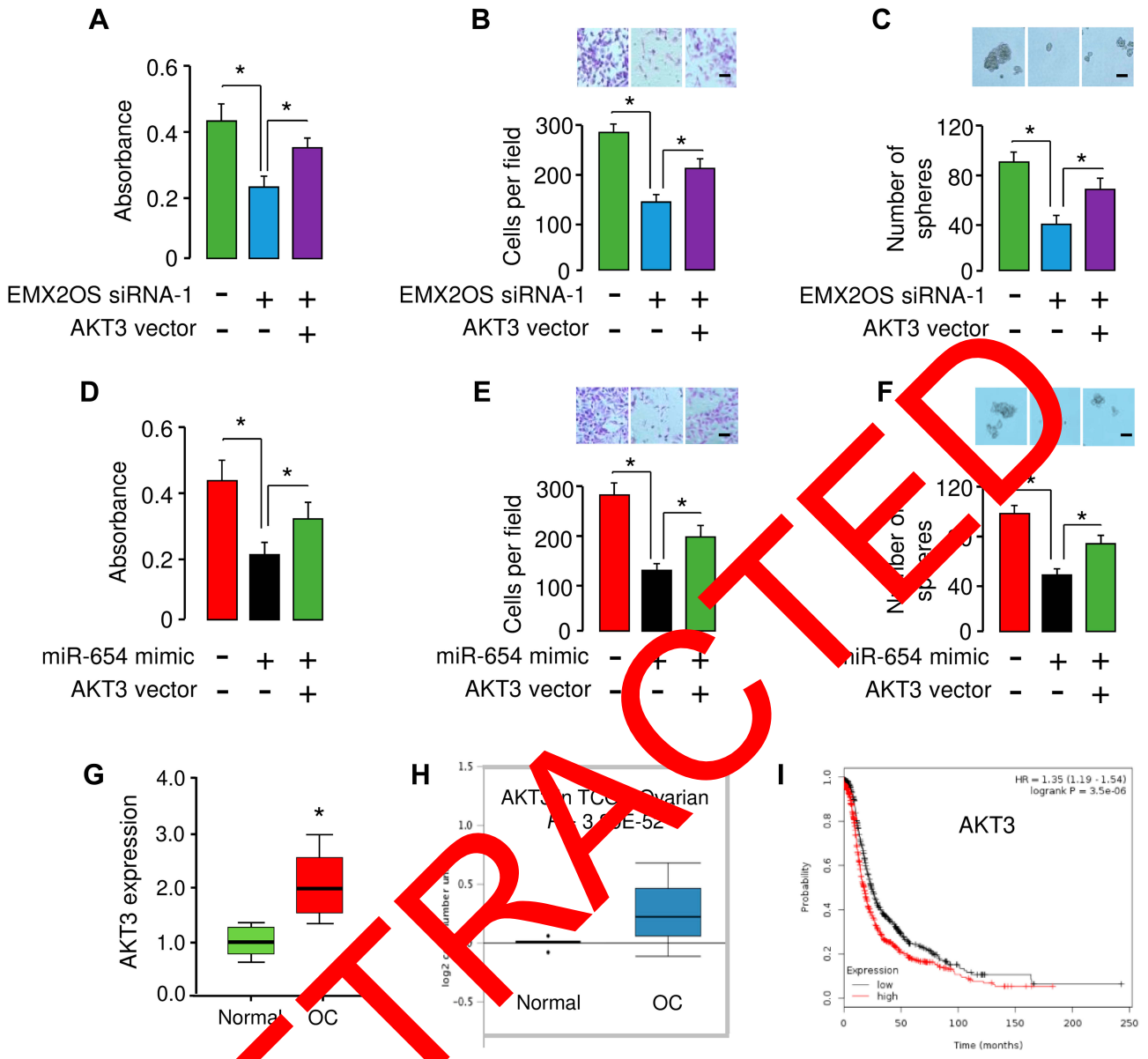

Figure 6 Introduction of AKT[illegible] everses th[illegible]hibitory effects of EMX2OS silencing and miR-654 overexpression in OC cells. (**A**–**C**) Proliferation (**A**), invasion (**B**) and sphere formation (**C**) of ES-2 cel[illegible]nsf[illegible]ed with EMX2OS siRNA or control siRNA, together with (or without) AKT3 vector. Scale bar: 50 μm in magnification × 100. (**D**–**F**) Proliferation (**D**), i[illegible]sion (**E**) [illegible]sphere form[illegible]on (**F**) of ES-2 cells transfected with miR-654 mimic or control mimic, together with (or without) AKT3 vector. Scale bar: 50 μm in magnif[illegible]ion [illegible]00. (**G**) [illegible]pressi[illegible]of AKT3 in OC samples (n = 50) and normal ovarian tissues (n = 50). (**H**) AKT3 expression in OC patients from Oncomine databa[illegible] (**I**) Kaplan[illegible]Meier curv[illegible]overall survival were created using the Kaplan–Meier Plotter with OC patients classified according to high and low AKT3 expression. *P<[illegible]5.
Abbreviation: [illegible]ovari[illegible]cancer.

Western blotting a[illegible]lysis demonstrated that PD-L1 was upregulated in OC cells compared with the normal ovary cell ISOE-80 (Figure 7A). We also overserved that deletion of AKT3 in ES-2 cells decreased PD-L1 protein expression, while overexpressing AKT3 upregulated PD-L1 levels in SKOV-3 cells (Figure 7B), implying that AKT3 acts upstream of PD-L1.

To determine whether PD-L1 was involved in the EMX2OS/miR-654/AKT3 axis-mediated OC cell prolifera tion, invasion and sphere formation, we next performed rescue experiments. ES-2 cells were co-transfected with EMX2OS siRNA, miR-654 mimic, or AKT3 siRNA, together with (or without) PD-L1 expression vector. We found that re-expression of PD-L1 was able to antagonize the inhibition of cell proliferation, invasion and sphere formation caused by EMX2OS knockdown, miR-654 overexpression, or AKT3 silencing (Figure 7C–K). Next, we sought to determine the expression of *PD-L1* mRNA levels in OC tissues and normal

tissues. Our qRT-PCR assays suggested that PD-L1 was highly upregulated in OC samples compared to normal samples (Figure 8A). Of importance, analysis of correlation between *PD-L1* expression and patient prognosis from microarray database revealed that PD-L1 overexpression was associated with poorer prognosis in OC patients (Figure 8B). Taken together, our results suggest that EMX2OS contributes to the malignant characteristics of OC cells through modulating the AKT3/PD-L1 axis by competitively binding with miR-654.

Discussion

Numerous studies have revealed that lncRNAs play critical roles in OC progression by acting as tumor suppressors or oncogenes.[18–20] For example, lncRNA NEAT1 and MALAT1 were reported to be upregulated in OC samples and were negative prognostic factors for OC.[18,19] The downregulation of lncRNA GAS5 was significantly associated with advanced clinical stage.[20] NEAT1 and GAS5 participated in the regulation of OC development through sponging tumor suppressor miRNAs.[18,20] However, little is known about the expression, function and underlying mechanisms of lncRNA EMX2OS in OC. In the current study, we demonstrated for the first time that EMX2OS expression was remarkably increased in OC tissues and OC cell lines. This result indicated that high expression may be associated with various pathological conditions in OC. Whether high EMX2OS expression was correlated with adverse clinical features, such as tumor stage, tumor size, and lymph node metastasis remains to be further explored.

In gain or loss-of-function assays, we demonstrated that EMX2OS overexpression had tumor-promoting effects to accelerate proliferation, invasion and sphere formation of ES-2 and OVCAR-3 cells. These results were consistent with the high abundance of EMX2OS in OC cells. Therefore, the silencing of EMX2OS might yield significant functional impact on these malignant properties of OC cells, suggesting that EMX2OS may be a novel therapeutic target for inhibiting OC progression.

LncRNAs could serve as competing endogenous RNAs by interacting with miRNAs and suppressing their functions in cancer.[18,20,21] In our study, we confirmed that EMX2OS could bind to miR-654 and suppressing its expression in OC. Importantly, miR-654 was reported to be a tumor suppressor in glioma.[22] Furthermore, we investigated whether miR-654 mediated the effects of EMX2OS in OC cell growth and invasion. Our data suggested that EMX2OS overexpression promoted OC cell proliferation and invasion, and the introduction of miR-654 could largely reverse these effects of EMX2OS. EMX2OS expression was negatively correlated with miR-654 expression in OC cell lines. Thus, EMX2OS might promote OC progression by inhibiting miR-654 expression.

Previous studies showed that AKT3 promotes tumor proliferation and invasion in seminoma, thyroid cancer, and liver cancer.[23–25] In prostate cancer cells lacking the tumor suppressor PTEN, the basal enzymatic activity of AKT3 was constitutively elevated and represented the major active AKT in these cells.[26] The same study also showed that the expression levels of AKT3 were significantly higher in the estrogen receptor-negative tumors in comparison to the estrogen receptor-positive tumors, indicating that AKT3 may contribute to the more aggressive clinical phenotype of prostate cancer.[26] Importantly, AKT3 is highly expressed in primary OCs, and specific downregulation of AKT3 expression resulted in marked inhibition of OC cell proliferation.[27] Consistent with these reports, we verified the oncogenic role of AKT3 in driving OC cell proliferation, and further demonstrated that its overexpression was critical for enhancing sphere formation and invasion of OC cells. Moreover, we confirmed that AKT3 was a direct and functional target of miR-654 in OC cells. Western blot analysis suggested that miR-654 negatively regulated the expression of AKT3 protein, and the level of miR-654 showed a reverse relationship with AKT3 in OC cells. In our rescue experiments, restoration of AKT3 abolished the effects of miR-654 in OC cells, demonstrating that AKT3 played important roles in mediating the EMX2OS/miR-654 axis-induced biological functions in OC.

Cancer growth and progression are associated with immune suppression. PD-L1 plays critical roles in evading anti-tumor immunity, and also actively promotes cancer initiation, epithelial-to-mesenchymal transition, metastasis, cancer stem cell properties, and resistance to therapy of various cancers through several tumor-intrinsic mechanisms.[28] High expression of PD-L1 was correlated with worse overall survival in multiple cancer types, including OC.[29] Tumor cell-intrinsic PD-L1 was shown to promote tumor-initiating cell generation in OC.[30] Our data provided the first demonstration that PD-L1 serves as a crucial downstream effector of AKT3, and targeting PD-L1 might possibly retard the initiation and progression of OC induced by the

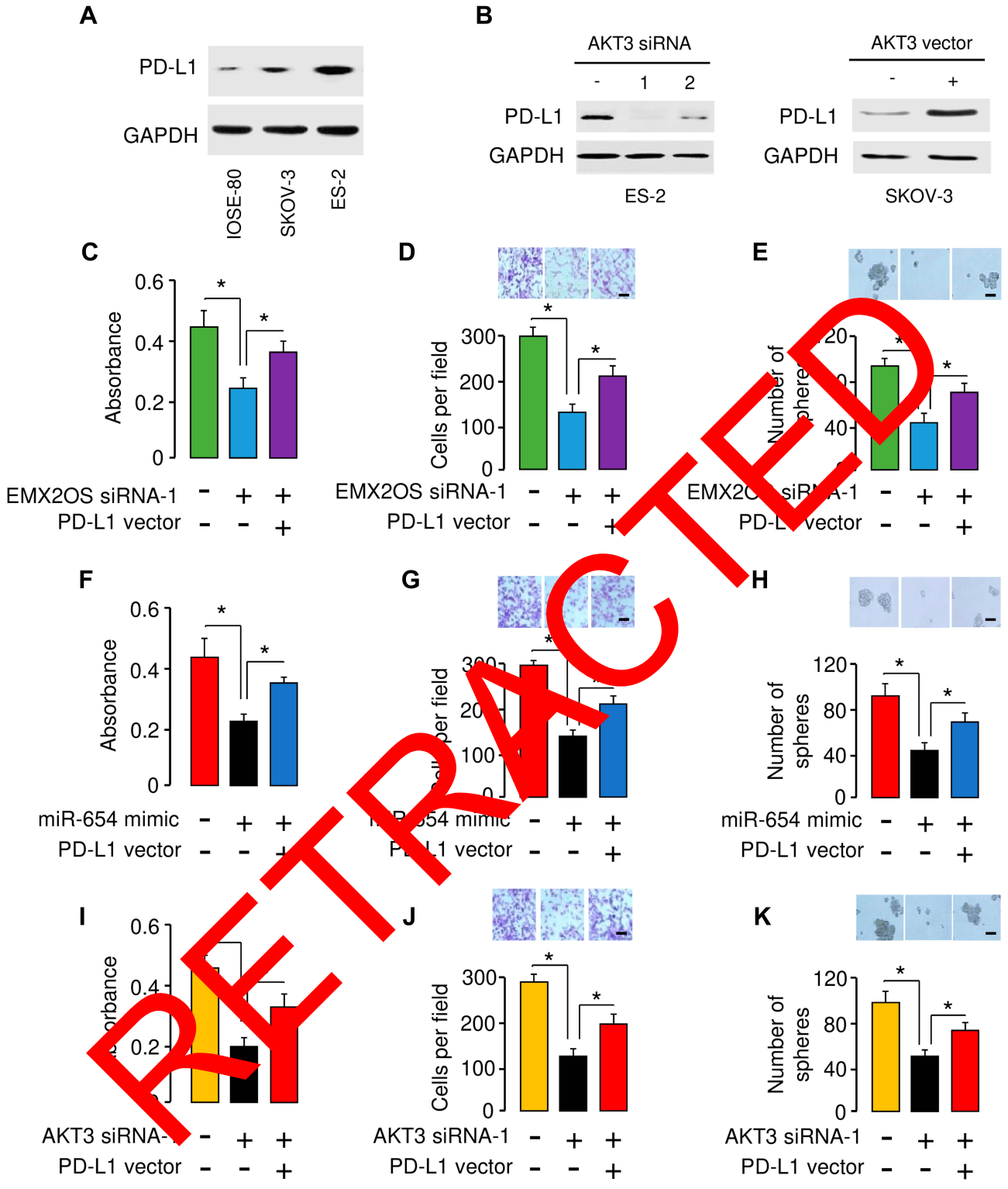

Figure 7 EMX2OS promoted OC cell proliferation, invasion and sphere formation via regulating the AKT3/PD-L1 axis by sponging miR-654. (**A**) Western blot analysis of PD-L1 in OC cell lines and normal ovary cell IOSE-80. (**B**) Western blot analysis of PD-L1 in ES-2 cells transfected with AKT3 siRNAs or control siRNA, and in SKOV-3 cells transfected with AKT3 vector or control vector. (**C, F, I**) Proliferation of ES-2 cells transfected with EMX2OS siRNA (**C**), miR-654 mimic (**F**) or AKT3 siRNA (**I**), together with (or without) PD-L1 vector. (**D, G, J**) Invasion of ES-2 cells transfected with EMX2OS siRNA (**D**), miR-654 mimic (**G**) or AKT3 siRNA (**J**), together with (or without) PD-L1 vector. Scale bar: 50 μm in magnification × 100. (**E, H, K**) Sphere formation ES-2 cells transfected with EMX2OS siRNA (**E**), miR-654 mimic (**H**) or AKT3 siRNA (**K**), together with (or without) PD-L1 vector. Scale bar: 50 μm in magnification × 100. *P<0.05.

Abbreviation: OC, ovarian cancer.

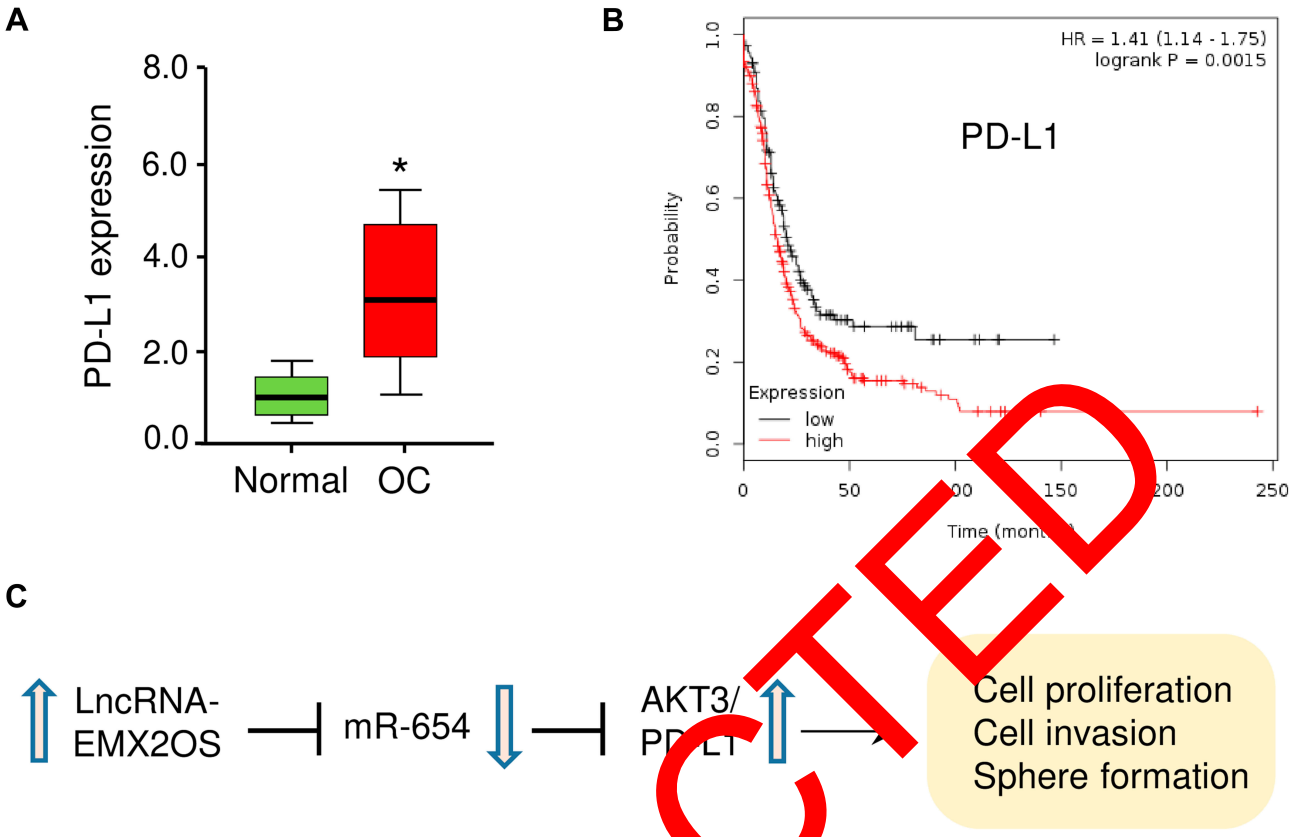

Figure 8 PD-L1 is overexpressed in OC and high PD-L1 expression was ...d with poor ...s of OC patients. (**A**) qRT-PCR analysis PD-L1 expression of in OC samples (n = 50) and normal ovarian tissues (n = 50). *P<0.05. (**B**) Kaplan–...ier cu... for overall survival were created using the Kaplan–Meier Plotter with OC patients classified according to high and low PD-L1 expression. (**C**) Schema illustrat... the m...hani...by which EMX2OS induces proliferation, invasion and sphere formation of ovarian cancer cells via regulating the miR-654-3p/AKT3/PD-L1 axis.
Abbreviation: OC, ovarian cancer.

EMX2OS/miR-654/AKT3 pathw..., alt...gh this possibility requires further investi...on.

Conclusion

Our data showed t...at EMX2OS served as a molecular sponge for miR-6...4, to ...upregulate the expression of AKT3 and P...L1, th...eby pr...oting the proliferation, invasion ...nd sph...re form...n of OC cells (Figure 8C). The E...X2OS/...-654/AKT3/PD-L1 pathway could be considered ... a potential target for the OC therapies in the future.

Acknowledgments

This work was supported by a grant from Jining No. 1 People's Hospital.

Author Contributions

All authors performed the experiments, contributed to data analysis, drafting and revising the article, gave final approval of the version to be published, and agree to be accountable for all aspects of the work.

Disclosure

The authors report no conflicts of interest in this work.

References

1. Torre LA, Trabert B, DeSantis CE, et al. Ovarian cancer statistics, 2018. *CA Cancer J Clin*. 2018;68(4):284–296. doi:10.3322/caac.21456
2. Balch C, Huang TH, Brown R, Nephew KP. The epigenetics of ovarian cancer drug resistance and resensitization. *Am J Obstet Gynecol*. 2004;191(5):1552–1572. doi:10.1016/j.ajog.2004.05.025
3. Siegel RL, Miller KD, Jemal A. Cancer statistics, 2016. *CA Cancer J Clin*. 2016;66(1):7–30. doi:10.3322/caac.21332
4. Liu J, Matulonis UA. New strategies in ovarian cancer: translating the molecular complexity of ovarian cancer into treatment advances. *Clin Cancer Res*. 2014;20(20):5150–5156. doi:10.1158/1078-0432.CCR-14-1312
5. Dong P, Xiong Y, Yue J, Hanley SJB, Watari H. miR-34a, miR-424 and miR-513 inhibit MMSET expression to repress endometrial cancer cell invasion and sphere formation. *Oncotarget*. 2018;9(33):23253–23263. doi:10.18632/oncotarget.25298

6. Dong P, Xiong Y, Yue J, et al. Long non-coding RNA NEAT1: a novel target for diagnosis and therapy in human tumors. *Front Genet*. 2018;9:471. doi:10.3389/fgene.2018.00471
7. Muhammad N, Bhattacharya S, Steele R, Ray RB. Anti-miR-203 suppresses ER-positive breast cancer growth and stemness by targeting SOCS3. *Oncotarget*. 2016;7:58595–58605. doi:10.18632/oncotarget.11193
8. Li H, Yu B, Li J, et al. Characterization of differentially expressed genes involved in pathways associated with gastric cancer. *PLoS One*. 2015;10(4):e0125013. doi:10.1371/journal.pone.0125013
9. Hough SR, Clements I, Welch PJ, Wiederholt KA. Differentiation of mouse embryonic stem cells after RNA interference-mediated silencing of OCT4 and Nanog. *Stem Cells*. 2006;24(6):1467–1475. doi:10.1634/stemcells.2005-0475
10. Dong P, Xiong Y, Hanley SJB, Yue J, Watari H. Musashi-2, a novel oncoprotein promoting cervical cancer cell growth and invasion, is negatively regulated by p53-induced miR-143 and miR-107 activation. *J Exp Clin Cancer Res*. 2017;36(1):150. doi:10.1186/s13046-017-0617-y.4
11. Tang Z, Li C, Kang B, Gao G, Li C, Zhang Z. GEPIA: a web server for cancer and normal gene expression profiling and interactive analyses. *Nucleic Acids Res*. 2017;45(W1):W98–W102. doi:10.1093/nar/gkx247
12. Liu F, Chen N, Gong Y, Xiao R, Wang W, Pan Z. The long non-coding RNA NEAT1 enhances epithelial-to-mesenchymal transition and chemoresistance via the miR-34a/c-Met axis in renal cell carcinoma. *Oncotarget*. 2017;8(38):62927–62938. doi:10.18632/oncotarget.17757
13. Jiang H, Huang G, Zhao N, et al. Long non-coding RNA TPT1-AS1 promotes cell growth and metastasis in cervical cancer via acting AS a sponge for miR-324-5p. *J Exp Clin Cancer Res*. 2018;37(1):169. doi:10.1186/s13046-018-0846-8
14. Yu H, Xu Y, Zhang D, Liu G. Long noncoding RNA LUCAT1 promotes malignancy of ovarian cancer through regulation [illegible] miR-612/HOXA13 pathway. *Biochem Biophys Res Commu* 2018;503(3):2095–2100. doi:10.1016/j.bbrc.2018.07.165
15. Xiao L, Wu J, Wang JY, et al. Long noncoding RNA uc.173 promotes renewal of the intestinal mucosa by inducing [illegible]gradation of MicroRNA 195. *Gastroenterology*. 201[illegible]154(3):5[illegible]–611. doi:10.1053/j.gastro.2017.10.009
16. Dong P, Xiong Y, Yue J, Hanley SJB, W[illegible]ari H[illegible]r-intrinsic PD-L1 signaling in cancer initiation, d[illegible]elopment a[illegible] treatment: beyond immune evasion. *Front On[illegible]*. [illegible]018;8:386. d[illegible]0.3389/fonc.2018.00386
17. Xue J, Chen C, Qi M, et al. Ty[illegible] Iγ phosphati[illegible]inositol phosphate kinase regulates PD-L1 expr[illegible]ion by activating [illegible]B. *Oncotarget*. 2017;8(26):42414–42427. doi:10.18632/oncotarget.17123
18. Yong W, Yu D, Jun Z, e[illegible]. Long [illegible]ncoding RNA NEAT1, regulated by LIN28B, promotes cell p[illegible]li[illegible]ation and [illegible]gration through sponging miR-506 in[illegible]rade s[illegible]us ovari[illegible] cancer. *Cell Death Dis*. 2018;9(9):86[illegible] doi:10.[illegible]38/s414[illegible]0[illegible]0908-z
19. Guo C, Wang X, Chen LP, et al. Long non-coding RNA MALAT1 regulates ovarian cancer cell proliferation, migration and apoptosis through Wnt/β-catenin signaling pathway. *Eur Rev Med Pharmacol Sci*. 2018;22(12):3703–3712. doi:10.26355/eurrev_201806_15249
20. Ma N, Li S, Zhang Q, Wang H, Qin H, Wang S. Long non-coding RNA GAS5 inhibits ovarian cancer cell proliferation via the control of microRNA-21 and SPRY2 expression. *Exp Ther Med*. 2018;16(1):73–82. doi:10.3892/etm.2018.6188
21. Salmena L, Poliseno L, Tay Y, Kats L, Pandolfi PP. A ceRNA hypothesis: the Rosetta Stone of a hidden RNA language? *Cell*. 2011;146(3):353–358. doi:10.1016/j.cell.2011.07.014
22. Jin P, Huang Y, Zhu P, Zou Y, Shao T, Wang O. CircRNA circHIPK3 serves as a prognostic marker to promote glioma progression by regulating miR-654/IGF2BP3 signaling. *Biochem Biophys Res Commun*. 2018;503(3):1570–1574. doi:10.1[illegible]rc.2018.07.081
23. Chen Y, Lu J, Xia L, et al. Testicular [illegible]phan rec[illegible]r 4 promotes tumor progression and implies poor [illegible]rvival through [illegible]KT3 regulation in seminoma. *Cancer Sci*. 2018;[illegible]9(2):384–394. [illegible]oi:10.1111/cas.13461
24. Lin Y, Cheng K, Wang [illegible]et al. miR-21[illegible]hibi[illegible] proliferation, migration, and invasio[illegible]via targ[illegible]g AKT3 [illegible] thyroid cancer. *Biomed Pharmacother*. 20[illegible];95:1718–1724. doi:10.1016/j.biopha.2017.09.07[illegible]
25. Yang H, Zheng [illegible]Shuai X, et a[illegible]Micro[illegible]NA-424 inhibits Akt3/E2F3 axis and t[illegible]or g[illegible]yth in hepato[illegible]ular carcinoma. *Oncotarget*. 2015;6(29):27736–27[illegible] doi:10.18632/oncotarget.4811
26. Nakat[illegible] Thompson [illegible] Barthel A, et al. Up-regulation of Akt3 in estrogen receptor-deficient breast cancers and androgen-independent prostate cancer lines. *J Biol Chem*. 1999;274([illegible]):21528–2153[illegible] doi:10.1074/jbc.274.31.21528
27. C[illegible]iano BE, Ch[illegible] JC, Hannan KM, et al. A specific role for AKT3 in th[illegible]nesis [illegible]ovarian cancer through modulation of G(2)-M phase transition. *Cancer Res*. 2006;66(24):11718–11725. doi:10.1158/0008-[illegible]CAN-06-1968
28. Dong P, Xiong Y, Yu J, et al. Control of PD-L1 expression by miR-140/142/340/383 and oncogenic activation of the OCT4-miR-18a pathway in cervical cancer. *Oncogene*. 2018;37(39):5257–5268. doi:10.1038/s41388-018-0347-4
29. Zhu J, Wen H, Bi R, Wu Y, Wu X. Prognostic value of programmed death-ligand 1 (PD-L1) expression in ovarian clear cell carcinoma. *J Gynecol Oncol*. 2017;28(6):e77. doi:10.3802/jgo.2017.28.e77
30. Gupta HB, Clark CA, Yuan B, et al. Tumor cell-intrinsic PD-L1 promotes tumor-initiating cell generation and functions in melanoma and ovarian cancer1. *Signal Transduct Target Ther*. 2016;1:16030. doi:10.1038/sigtrans.2016.30